ChemComm

Molybdenum Sulphide Clusters as Redox Active Supports for Low-Valent Uranium

Journal:	*ChemComm*
Manuscript ID	CC-COM-11-2023-005561.R1
Article Type:	Communication

ARTICLE

Molybdenum Sulphide Clusters as Redox Active Supports for Low-Valent Uranium

Received 00th January 20xx,
Accepted 00th January 20xx

DOI: 10.1039/x0xx00000x

Kamaless Patra, William W. Brennessel, and Ellen M. Matson*

The preparation of an actinide substituted cubane cluster, $(Cp^*_3Mo_3S_4)Cp^*UI_2$, and its reduced derivatives are reported. Structural and spectroscopic investigations provide insight into the unique interactions between the actinide and its redox-active molybdenum sulfide metalloligand, serving as a model to study atomically-dispersed, low-valent actinide ions on MoS_2 surfaces. To probe the ability of the assembly to facilitate multielectron small molecule activation, the reactivity of the fully-reduced cluster, $(Cp^*_3Mo_3S_4)Cp^*U$, with azobenzene was investigated. Addition of the substrate results in the formation of a *cis* - bis-imido cluster, $(Cp^*_3Mo_3S_4)Cp^*U(=NPh)_2$. Cooperative reactivity between the actinide and redox-active support facilitates the 4 e- reduction of substrate.

The chemical and electronic interactions between actinide ions and redox-active surfaces is an important area of research, with implications in nuclear separations and catalysis.[1-3] A class of materials that has recently emerged as an intriguing platform for actinide ions are Group(VI) chalcogenides (e.g. MoS_2, WS_2; Figure 1).[4] These materials have demonstrated great promise in the context of the extraction of uranium from sea water. Results have emphasized the benefit of soft-soft interactions between the sulphur donors and uranium atoms to promote selectivity of uranium uptake over harder impurity ions, as well as for enhanced electronic communication between the material and the actinide ion.[5-12]

The unique interactions between uranium and MoS_2 surfaces motivated our interest in the synthesis of molecular analogues to model uranium uptake and reactivity at a redox active support. Studying low-valent uranium on a redox-active surface will also allow us to model the reactivity of similar composites toward small-molecule activation. In this work, we demonstrate that molybdenum sulphide hemi-cubane clusters of the formula $Cp^*_3Mo_3S_4^{n+}$ serve as redox-active ligands for low-valent uranium, effectively modelling interactions of the basal plane of MoS_2 with reduced actinide ions. The use of $Cp^*_3Mo_3S_4^{n+}$ as a tripodal metalloligand for transition metals has previously been reported; in a series of manuscripts, Ohki and co-workers have described the synthesis of $Cp^*_3Mo_3S_4M$ complexes, where M = transition metals ranging from Group IV to Group X.[13, 14] Of most relevance to this work, in the case of iron and titanium adducts of the thiomolybdate cluster, N_2 fixation has been demonstrated, with significant contributions of reducing equivalents stored at the "Mo_3S_4" core.[15, 16]

To install a single actinide centre at the surface of the molybdenum sulphide hemi-cubane, we opted to explore the coordination chemistry of $Cp^*UI_2(THF)_3$ with **$Cp^*_3Mo_3S_4$**. We hypothesized that the presence of the ancillary cyclopentadienide ligand on uranium would prevent formation of sandwich-type clusters that would limit subsequent investigations into the reactivity of the actinide centre. Addition of $Cp^*UI_2(THF)_3$ to **$Cp^*_3Mo_3S_4$** in toluene results in immediate dissolution of the semi-soluble starting materials and a colour

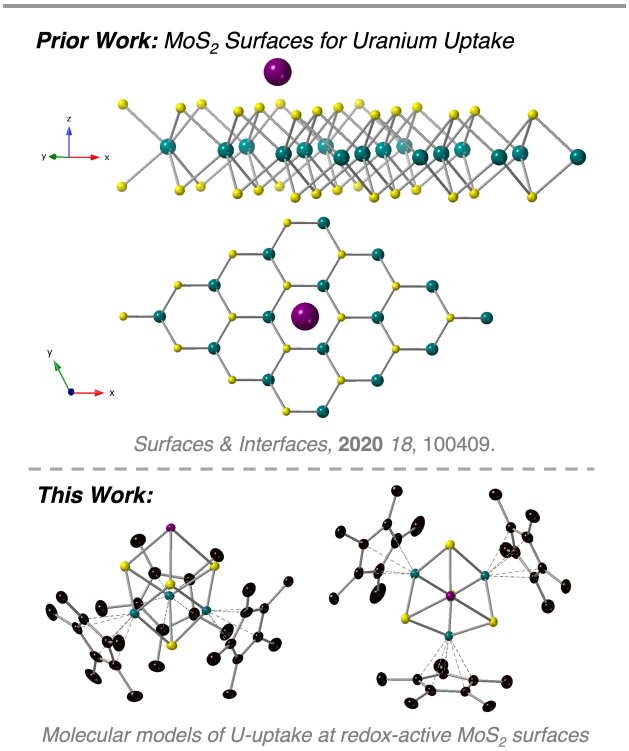

Figure 1. Uranium uptake on MoS_2 surfaces. Prior DFT model predicted for U(VI) adsorbed on MoS_2 (top). Molecular models of uranium uptake at MoS_2 surfaces (bottom).

[a] *Department of Chemistry, University of Rochester, Rochester NY 14627 USA.*
Electronic Supplementary Information (ESI) available: Experimental details, including compound preparations and characterization data. Crystallographic data for **$(Cp^*_3Mo_3S_4)Cp^*UI_2$** (CCDC 2306643), **$(Cp^*_3Mo_3S_4)Cp^*UI$** (CCDC 2306644), **$Cp^*_3Mo_3S_4Cp^*U(=NPh)_2$** (CCDC 2306645). See DOI: 10.1039/x0xx00000x

Scheme 1. Synthesis of **$(Cp^*_3Mo_3S_4)Cp^*UI_2$** and sequential chemical reduction to generate **$(Cp^*_3Mo_3S_4)Cp^*UI$** and **$(Cp^*_3Mo_3S_4)Cp^*U$**.

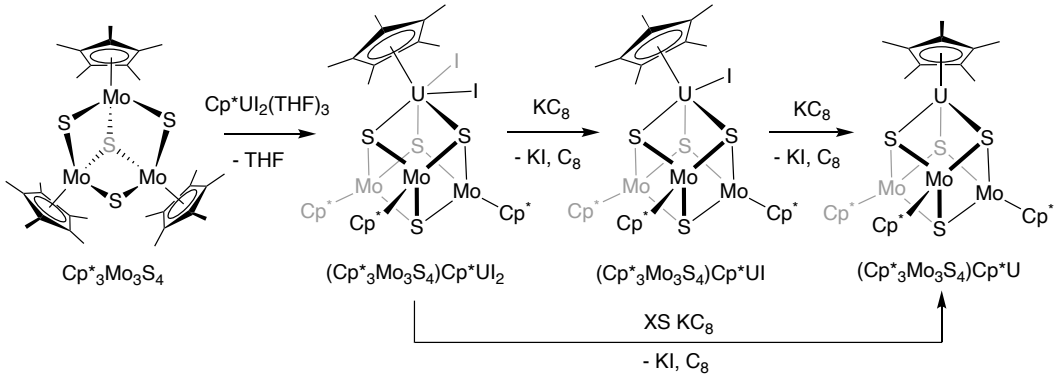

change to brown-green. Volatiles were removed under reduced pressure, leaving a brown crystalline solid. Initial characterization of the reaction product by ^{1}H NMR spectroscopy reveals two singlets with a 3:1 intensity ratio, consistent with formation of the anticipated product, **$(Cp^*_3Mo_3S_4)Cp^*UI_2$** (Figure S3). The signal corresponding to protons of the Mo-bound Cp* ligands (δ = 4.45 ppm) is shifted upfield in comparison to the starting material, **$Cp^*_3Mo_3S_4$** (δ = 8.59 ppm), indicating that the protons of the metalloligand are more shielded upon product formation. In contrast, the methyl protons of U-Cp* (δ = 7.39 ppm) are shifted downfield in comparison to $Cp^*UI_2(THF)_3$ (δ = 1.78 ppm), suggesting the actinide centre becomes electron deficient upon coordination to **$Cp^*_3Mo_3S_4$**.[17, 18] We hypothesize that the observed changes in electron shielding/de-shielding of the methyl protons on the Cp* ligand(s) is a result of electron transfer from the low-valent uranium centre to $Cp^*_3Mo_3S_4$ upon complexation.

Unambiguous confirmation of the identity of the product was performed by single crystal X-ray diffraction (SCXRD; Figure 2, Tables S2). Crystals of **$(Cp^*_3Mo_3S_4)Cp^*UI_2$** suitable for X-ray analysis were grown from a concentrated solution of the product in benzene. Refinement of the data indicates coordination of the low-valent uranium centre to the trisulfide-face of the metalloligand. The observed binding mode effectively models coordination of actinide centres to the basal plane of MoS_2 proposed by density functional theory.[7-9]

Support for charge transfer from the actinide to the molybdenum sulphide metalloligand upon formation of **$(Cp^*_3Mo_3S_4)Cp^*UI_2$** is obtained through inspection of bond distances. The U-I bond lengths in **$(Cp^*_3Mo_3S_4)Cp^*UI_2$** (3.0681(3), 3.0825(3) Å) are considerably shorter than those reported for the starting material, $Cp^*UI_2(THF)_3$ (3.161(1), 3.179(1) Å), resembling more closely values reported for U(IV) complexes (U^{IV}-I: 2.9588(10) – 3.1045(10) Å; average = 3.06 Å).[18-22] Changes are also observed in the bonding of the metalloligand that indicate reduction of the molybdenum sulphide assembly. The Mo-μ_2S (avg) distance of the neutral metalloligand (**$Cp^*_3Mo_3S_4$**) is 2.309 Å,[23] while in **$(Cp^*_3Mo_3S_4)Cp^*UI_2$**, this distance (Mo-μS_U (avg)) is elongated to 2.3644 Å. The observed Mo-μS_U distances resemble those reported for the potassium adduct of the 1e$^-$ reduced assembly, $[(Cp^*Mo)_3S_4]^-K^+$(18-C-6) (Mo-μS_K (avg) = 2.343 Å).[13] Moreover, the Mo-μS_{Mo} (avg) distance (2.3644 Å) and mean Mo-Mo distance (2.8776 Å) are similar to those reported for $[(Cp^*Mo)_3S_4]^-K^+$(18-C-6) (Mo-μS_{Mo} (avg) = 2.343 Å, Mo-Mo (avg) = 2.8553 Å).[13] Collectively these results support the hypothesis

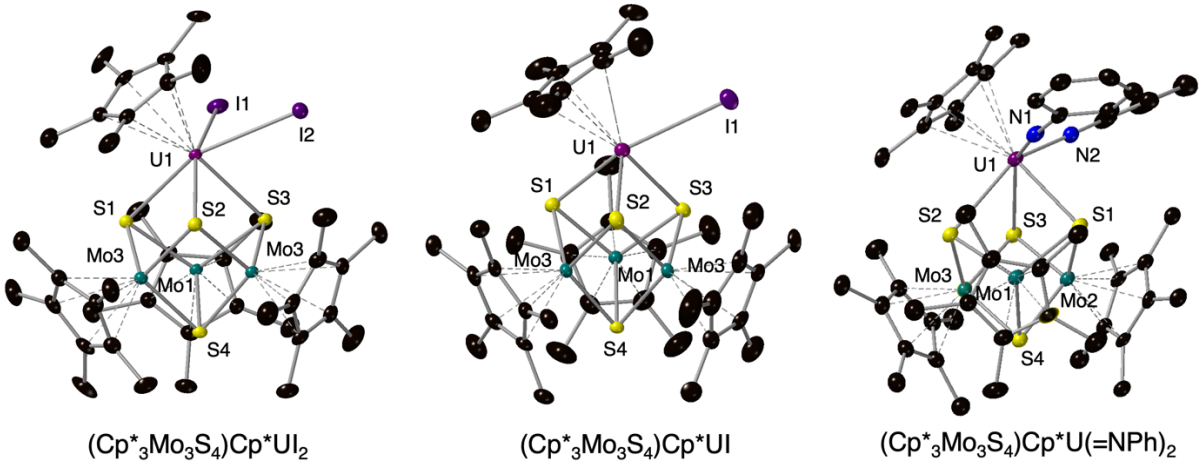

Figure 2. Molecular structures of **$(Cp^*_3Mo_3S_4)Cp^*UI_2$** (left), **$(Cp^*_3Mo_3S_4)Cp^*UI$** (middle), and **$(Cp^*_3Mo_3S_4)Cp^*U(=NPh)_2$** (right) are shown with 30% probability ellipsoids. Solvent molecules and hydrogen atoms included in the unit cell have been removed for clarity. Key: black ellipsoids, C; blue ellipsoids, N; yellow ellipsoids, S; purple ellipsoids, I; aquamarine ellipsoids, Mo; magenta ellipsoids, U.

that electron transfer is an important factor in promoting binding of the actinide ion to the metal chalcogenide metalloligand.

Following isolation of **(Cp*$_3$Mo$_3$S$_4$)Cp*UI$_2$**, our attention turned to the reduction of the heterometallic assembly (Scheme 1). Addition of 2.2 equiv. of potassium graphite (KC_8) to a toluene solution of **(Cp*$_3$Mo$_3$S$_4$)Cp*UI$_2$** results in the formation of the mono-reduced assembly, **(Cp*$_3$Mo$_3$S$_4$)Cp*UI**, in good yield (65 %). **(Cp*$_3$Mo$_3$S$_4$)Cp*UI** was initially characterized by ^{1}H NMR spectroscopy; the spectrum of the reduced assembly exhibits a comparable pattern to that of **(Cp*$_3$Mo$_3$S$_4$)Cp*UI$_2$**, with a downfield shift of the resonances assigned to the Cp*-methyl protons of the ancillary ligands bound to both molybdenum (δ = 4.88 ppm) and uranium (δ = 8.05 ppm) centres (Figure S6). The molecular structure of **(Cp*$_3$Mo$_3$S$_4$)Cp*UI** was confirmed by SCXRD (see below). Addition of 4.4 equiv of KC_8 to **(Cp*$_3$Mo$_3$S$_4$)Cp*UI$_2$** results in the formation of a distinct product, identified as the di-reduced assembly, **(Cp*$_3$Mo$_3$S$_4$)Cp*U** (Yield = 61 %). The ^{1}H NMR spectrum of **(Cp*$_3$Mo$_3$S$_4$)Cp*U** possesses two major resonances with a 3:1 ratio, corresponding to the methyl-protons of the Cp* ligands bound to molybdenum and uranium, respectively. Notably, there is a striking upfield shift observed for both signals in comparison to those observed in the ^{1}H NMR spectra of **(Cp*$_3$Mo$_3$S$_4$)Cp*UI$_2$** and **(Cp*$_3$Mo$_3$S$_4$)Cp*UI** (Figure S7; Cp*$_{Mo}$ = -0.44 ppm; Cp*$_U$ = -7.89 ppm). Independent synthesis of **(Cp*$_3$Mo$_3$S$_4$)Cp*U** is accomplished via addition of 2.2 equiv of KC_8 to **(Cp*$_3$Mo$_3$S$_4$)Cp*UI** (Yield = 64 %), providing support for the formation of the suggested product. Unfortunately, attempts to crystallize **(Cp*$_3$Mo$_3$S$_4$)Cp*U** have thus far been unsuccessful, preventing its characterization by SCXRD.

Analysis of structural data obtained via X-ray diffraction of single crystals of **(Cp*$_3$Mo$_3$S$_4$)Cp*UI** offers insight into changes in interactions between the actinide centre and the redox active support upon reduction (Figure 2, Table S2). The coordination environment of the uranium centre is composed of a single iodide moiety, the η_5-Cp* ligand, and the three sulphide atoms of the face of the hemi-cubane scaffold. The U-S bond distances range from 2.6300(14) – 2.7012(17) Å, substantially shortened from the values observed in **(Cp*$_3$Mo$_3$S$_4$)Cp*UI$_2$** (U-S: 2.7724(11) – 2.7770(10) Å). We inspected the distance between the uranium centre and the centroid defining the plane of three μ^2-bridged sulphur centre of **Cp*$_3$Mo$_3$S$_4$** (S_{surf}) to quantify the extent of interaction between the actinide and metalloligand. In **(Cp*$_3$Mo$_3$S$_4$)Cp*UI$_2$**, the uranium centre is situated at a distance of 1.8554(6) Å away from the [MoS] surface. Consistent with the shortening of the U-S contacts, this distance decreases substantially upon formation of **(Cp*$_3$Mo$_3$S$_4$)Cp*UI** (U-S_{surf} = 1.6623 (9) Å). This observation indicates a stronger interaction between actinide and metalloligand following reduction.

Considering the significance of work in understanding actinide uptake on redox-active surfaces, the bond metrics of **(Cp*$_3$Mo$_3$S$_4$)Cp*UI$_2$** and **(Cp*$_3$Mo$_3$S$_4$)Cp*UI** have been compared with those modelled for uranyl uptake on MoS_2 surfaces, irrespective of the ancillary ligand bound to uranium. While in both cases, the uranium centre binds to cluster surface in a mode similar to that predicted for uranyl binding at the basal plane of MoS_2, the contacts between the model of the MoS_2 surface and the uranium centre are much shorter than predicted for UO_2^{2+} and MoS_2.[6-8] These observations indicate a more robust interaction between uranium and the molecular model of the [MoS] surface. We hypothesize this is due to discrepancies in oxidation state of the uranium ions; the low-valent uranium centres investigated in this work bind more strongly to the surface of the metalloligand. This hypothesis is supported by the shortening of contacts between uranium and **Cp*$_3$Mo$_3$S$_4$** upon reduction of the assembly. Indeed, recent reports describe the utility of an applied potential for improved extraction of uranyl ions at exceptionally dilute concentrations (~100 ppm).[7] Application of a positive voltage facilitates the release of the uranium centre from MoS_2, leveraging electro-swing technologies for purification of uranium from sea water samples. Similarly, our results suggest reduction of either the actinide or MoS_2 materials will serve to increase the affinity of the surface for actinide ions, improving sequestration strategies for uranium ions.

With the low-valent uranium adducts of the redox active metalloligand in hand, our attention turned to the investigation of the multielectron reactivity of the system. Initial experiments explored the addition of azobenzene to the fully reduced form of the cluster, **(Cp*$_3$Mo$_3$S$_4$)Cp*U** (Scheme 2). We hypothesized that this reaction would serve as an excellent probe of cooperative reactivity of the metalloligand and actinide centre, modelling small molecule activation of atomically dispersed uranium centres at the surface of redox-active supports. The ^{1}H-NMR spectrum of the crude reaction mixture revealed quantitative conversion of starting materials to a single product. Signals corresponding to the methyl protons of the Mo-Cp* (9.77 ppm, 45 H) and U-Cp* (3.63 ppm, 15 H) are shifted downfield in comparison to the starting material (Figure S9), consistent with oxidation of the cluster. Three additional resonances are observed at 6.63, 6.46, and 5.91 ppm, suggesting formation of phenyl imido substituents at the actinide centre following activation of the substrate.

Scheme 2. Synthesis of **(Cp*$_3$Mo$_3$S$_4$)Cp*U(=NPh)$_2$**.

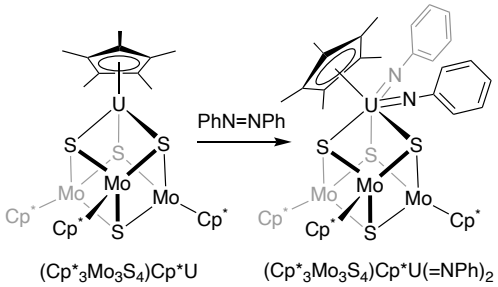

The formation of the anticipated bis-imido product, **(Cp*$_3$Mo$_3$S$_4$)Cp*U(=NPh)$_2$**, was confirmed via SCXRD (Figure 2, Table S2). The molecular structure of **(Cp*$_3$Mo$_3$S$_4$)Cp*U(=NPh)$_2$** reveals complete cleavage of the N=N bond of azobenzene, resulting in the formation of two phenyl imido substituents bound to the uranium centre. The imido moieties are positioned in a *cis* geometry (<N-U-N = 99.1(4)°), with U=N bond distances of 2.024(8) and 2.015(9) Å. The U=N bond distances are similar

to values reported for high-valent uranium-bis(imido) complexes (1.950(7) – 2.047(8) Å).[24-27] Most significantly, the U-S_{surf} distance increases substantially upon oxidation of the assembly (U-S_{surf} = 2.0187 (15) Å); the U-S_{surf} distance of **(Cp*$_3$Mo$_3$S$_4$)Cp*U(=NPh)$_2$** resembles more closely predicted contacts between the uranyl ion and MoS_2 (UO_2^{2+}-S_{surf} = 2.47 Å).

The activation of azobenzene by low-valent uranium complexes supported by redox-active ligands has been observed previously. Most similar to the studies reported here, Bart and co-workers have described the formation of a series of uranium bis-imido complexes following addition of azobenzene to Cp*U(PDI)(THF) complexes (PDI = 2,6-diiminopyridine).[28] In both examples, reduction of the substrate is facilitated by cooperative reactivity of the redox active ligand and uranium centre. However, a notable difference between these two examples lies in the relative positions of the imido substituents following azobenzene activation. In the case of $Cp^RU(=NPh)_2(PDI)$, the imido moieties are located *trans* to one another; the inverse trans influence operative in actinide complexes results in shortening of the U=N bonds. By comparison, the three-dimensional structure of the molybdenum sulphide metalloligand enforces a *cis* arrangement of the imido moieties, resulting in elongation of the U=N bonds. This result translates to imido substituents that are substantially activated and poised for further reactivity.

In summary, we report the synthesis and characterization of low-valent uranium complexes supported by a redox-active molybdenum sulphide metalloligand. Our results indicate the extent of interaction between the actinide centre and the metalloligand increases as the cluster is reduced, providing insight into strategies of electrochemically cyclable actinide uptake at the basal plane of Group(VI) chalcogenide surfaces. Furthermore, our foray into the reactivity of the reduced form of our cluster, **(Cp*$_3$Mo$_3$S$_4$)Cp*U**, with azobenzene models the reactivity of reduced uranium atoms deposited on redox active supports. The cleavage of the N=N bond of azobenzene by the reduced form of the cluster, **(Cp*$_3$Mo$_3$S$_4$)Cp*U**, results in the formation of a uranium bis-imido product, **(Cp*$_3$Mo$_3$S$_4$)Cp*U(=NPh)$_2$**, providing evidence for cooperative reactivity between the metalloligand and actinide centre. Indeed, by storing electron density in the molybdenum sulphide metalloligand, uranium functions as a U(I) or U(II) synthon and delivers four electrons to substrate. Ongoing investigations focus on probing the implications of the cis-geometry of the bis-imido product in catalysis, as well as the full scope of reactivity of the reduced assembly with small molecule substrates.

Financial support for this work was provided by the U.S. Department of Energy, Office of Basic Energy Sciences Heavy Element Program, under award DE-SC0020436. The authors would like to acknowledge Leyla Valerio for helpful discussions during the development of this project and feedback during preparation of the manuscript.

Author Contributions

K.P. synthesized and characterized all compounds. E.M.M. directed the research project and obtained funding. W.W.B. determined the crystal structures. The manuscript was written through contributions of all authors, and all authors have given approval of the final version of the manuscript.

Conflicts of interest

There are no conflicts to declare.

Notes and references

1 M. B. Jones and A. J. Gaunt, *Chem. Rev.*, 2013, **113**, 1137-1198.
2 L. S. Natrajan, A. N. Swinburne, M. B. Andrews, S. Randall and S. L. Heath, *Coord. Chem. Rev.*, 2014, **266-267**, 171-193.
3 D. R. Hartline and K. Meyer, *JACS Au*, 2021, **1**, 698-709.
4 X. Zhang and Y. Liu, *Environ. Sci. Nano*, 2020, **7**, 1008-1040.
5 S. Singh, S. Sharma, B. S. Bajwa and I. Kaur, *J. Environ. Chem. Eng.*, 2022, **10**, 108883.
6 Y. Liu, C. Fang, S. zhang, W. Zhong, Q. Wei, Y. Wang, Y. Dai, Y. Wang, Z. Zhang and Y. Liu, *Surf. Interfaces*, 2020, **18**, 100409.
7 X. Tang, Y. Liu, M. Liu, H. Chen, P. Huang, H. Ruan, Y. Zheng, F. Yang, R. He and W. Zhu, *Nanoscale*, 2022, **14**, 6285-6290.
8 Y. Zhang, Y. Jiang, S. Bai, Z. Dong, X. Cao, Q. Wei, Y. Wang, Z. Zhang and Y. Liu, *Journal of Hazardous Materials*, 2023, **457**, 131745.
9 X. Li, Q. Li, W. Linghu, R. Shen, B. Zhao, L. Dong, A. Alsaedi, T. Hayat, J. Wang and J. Liu, *Environ. Tech. Innov.*, 2018, **11**, 328-338.
10 B.-M. Jun, H.-K. Lee, S. Park and T.-J. Kim, *Separation and Purification Technology*, 2021, **278**, 119675.
11 A. C. Sutorik and M. G. Kanatzidis, *J. Am. Chem. Soc.*, 1997, **119**, 7901-7902.
12 M. J. Manos and M. G. Kanatzidis, *J. Am. Chem. Soc.*, 2012, **134**, 16441-16446.
13 Y. Ohki, K. Uchida, R. Hara, M. Kachi, M. Fujisawa, M. Tada, Y. Sakai and W. M. C. Sameera, *Chem.*, 2018, **24**, 17138-17147.
14 I. Takei, K. Suzuki, Y. Enta, K. Dohki, T. Suzuki, Y. Mizobe and M. Hidai, *Organometallics*, 2003, **22**, 1790-1792.
15 Y. Ohki, K. Munakata, Y. Matsuoka, R. Hara, M. Kachi, K. Uchida, M. Tada, R. E. Cramer, W. M. C. Sameera, T. Takayama, Y. Sakai, S. Kuriyama, Y. Nishibayashi and K. Tanifuji, *Nature*, 2022, **607**, 86-90.
16 Y. Ohki, K. Uchida, M. Tada, R. E. Cramer, T. Ogura and T. Ohta, *Nat. Comm.*, 2018, **9**, 3200.
17 M. Roger, L. Belkhiri, T. Arliguie, P. Thuéry, A. Boucekkine and M. Ephritikhine, *Organometallics*, 2008, **27**, 33-42.
18 S. A. Pattenaude, C. S. Kuehner, W. L. Dorfner, E. J. Schelter, P. E. Fanwick and S. C. Bart, *Inorg. Chem.*, 2015, **54**, 6520-6527.
19 N. H. Anderson, S. O. Odoh, Y. Yao, U. J. Williams, B. A. Schaefer, J. J. Kiernicki, A. J. Lewis, M. D. Goshert, P. E. Fanwick, E. J. Schelter, J. R. Walensky, L. Gagliardi and S. C. Bart, *Nat. Chem.*, 2014, **6**, 919-926.
20 E. M. Matson, S. M. Franke, N. H. Anderson, T. D. Cook, P. E. Fanwick and S. C. Bart, *Organometallics*, 2014, **33**, 1964-1971.
21 M. J. Monreal, R. K. Thomson, T. Cantat, N. E. Travia, B. L. Scott and J. L. Kiplinger, *Organometallics*, 2011, **30**, 2031-2038.
22 C. R. Groom, I. J. Bruno, M. P. Lightfoot and S. C. Ward, *Acta Cryst. B Struct Sci Cryst Eng Mater*, 2016, **72**, 171-179.
23 R. E. Cramer, K. Yamada, H. Kawaguchi and K. Tatsumi, *Inorg. Chem.*, 1996, **35**, 1743-1746.
24 R. E. Jilek, L. P. Spencer, R. A. Lewis, B. L. Scott, T. W. Hayton and J. M. Boncella, *J. Am. Chem. Soc.*, 2012, **134**, 9876-9878.
25 S. C. Bart, C. Anthon, F. W. Heinemann, E. Bill, N. M. Edelstein and K. Meyer, *J. Am. Chem. Soc.*, 2008, **130**, 12536-12546.
26 I. Castro-Rodriguez, K. Olsen, P. Gantzel and K. Meyer, *J. Am. Chem. Soc.*, 2003, **125**, 4565-4571.
27 B. P. Warner, B. L. Scott and C. J. Burns, *Angew. Chem. Int. Ed.*, 1998, **37**, 959-960.
28 D. P. Cladis, J. J. Kiernicki, P. E. Fanwick and S. C. Bart, *Chem. Commun.*, 2013, **49**, 4169-4171.